

# Translational diffusion of 12-arm star polystyrenes in dilute and concentrated poly(vinyl methyl ether) solutions

T. P. Lodge\* and P. Markland

*Department of Chemistry, University of Minnesota, Minneapolis, MN 55455, USA*

*(Received 2 October 1986; accepted 17 November 1986)*

The technique of dynamic light scattering from isorefractive ternary solutions has been used to study the translational diffusion behaviour of 12-arm star polystyrenes (PS) in dilute and concentrated solutions of poly(vinyl methyl ether) (PVME). PS molecular weights ranged from  $5.5 \times 10^4$  to  $1.69 \times 10^6$ . The PVME molecular weight was  $1.4 \times 10^5$ , and the PVME concentration was varied from 0.001 to  $0.30 \text{ g ml}^{-1}$ . The concentration dependence of diffusion is well described by the functional form  $D/D_0 = \exp(-ac^u)$ , although there is some evidence that the star dimensions decrease with increasing PVME concentration. Comparison with the diffusion behaviour of linear PS in PVME solutions suggests that, for these molecular weights of PS and PVME, the diffusant topology is not important, and thus reptation is not a significant mechanism under these conditions. At the same time, neither the Stokes-Einstein relation nor a simple scaling function,  $f(R/\xi)$ , can describe the observed behaviour. These results are interpreted as reflecting substantial PVME mobility, relative to the PS stars.

(Keywords: diffusion; branching; light scattering)

## INTRODUCTION

The effect of long-chain branching on the static and dynamic properties of polymer liquids continues to be an area of great interest. Advances in synthetic methodology have resulted in the availability of model branched molecules with carefully controlled topology and molecular weight. Star-branched polymers have proven to be particularly useful, and a range of both functionality and chemical structure is accessible. Star polymers provide a means to investigate many important issues, especially those concerning polymer dynamics in concentrated solutions and melts. For example, in the limit of long branches and small numbers of arms, the translational diffusion coefficient for stars in linear or branched polymer matrices can test the related hypotheses of reptation and constraint release, through comparison with linear polymer diffusion coefficients. At the other extreme, stars with many short branches, the diffusion process may be similar to that for spherical particles, and thus can be used as a probe of hydrodynamic interactions in polymer solutions, or as a non-electrolyte model for globular protein mobility.

For a star polymer diffusing through a fixed matrix, such as a crosslinked network, de Gennes has shown that the entangled arms should lead to an exponential dependence of the diffusion coefficient on molecular weight, in contrast to the inverse-square dependence predicted for reptating linear molecules<sup>1</sup>. In a concentrated solution or melt, where the obstacles are not fixed, effective suppression of reptation by long-chain branching may increase the relative importance of the constraint release mechanism, as has been considered in detail by Klein<sup>2</sup>. Thus, the diffusion properties of linear

and star polymers in concentrated solutions and melts should permit assessment of the relative contributions of reptation, constraint release, or other possible mechanisms. If reptation and/or constraint release are indeed significant in entangled solutions, then it is desirable to establish the solution conditions where reptation becomes important. This issue has been addressed by considering diffusion of linear polymers in the semi-dilute regime, but as yet is not resolved. In the dilute to semi-dilute crossover region, the physical picture is quite complicated, and it appears that no simple physical picture will suffice.

Extensive measurements of spherical probe particle diffusion in semi-dilute linear polymer solutions have suggested an empirical expression for the diffusion coefficient which is similar to that obtained by considering the concentration dependence of interchain hydrodynamic interactions<sup>3</sup>. Surprisingly, to some degree diffusion behaviour of linear polymers appears to be describable via the same functional form<sup>4</sup>. Thus, there is a definite need for additional experimental insight into the factors governing polymer diffusion beyond the dilute solution regime. One promising route is to compare the diffusion behaviour of linear and branched polymers in identical matrices. If reptation becomes important, a substantial retardation of branched polymer mobility relative to linear polymers of comparable dimension is expected. Conversely, if the apparent ability of a single functional form to describe the diffusion of both linear chains and spherical particles reflects universality of the diffusion mechanism, little difference between branched and linear polymers should be observed. With the exception of recent studies of three-arm star diffusion in melts<sup>5-7</sup> and semi-dilute ternary solutions<sup>8</sup>, few diffusion data have been reported for star-branched polymers beyond the dilute solution regime. In general, the melt

\* To whom correspondence should be addressed

data indicate a suppression of branched polymer mobility, in accordance with the reptation picture. At the other limit, in dilute solution, the extensive pulsed field gradient n.m.r. measurements of von Meerwall *et al.*<sup>9-11</sup> on linear and branched polystyrenes, polyisoprenes and polybutadienes were conducted in non-entangled binary solutions, so that immediate comparison of the diffusion properties for different topologies in the same matrix was not possible. However, their results did on occasion tend into the semi-dilute regime, and no substantial difference between linear and branched polymer mobility is observed. Thus, at intermediate concentrations a transition from topology-independent to topology-dependent diffusion mechanisms should be observed. In this work, the technique of dynamic light scattering in isorefractive ternary solutions has been employed to measure the translational diffusion of 12-arm polystyrene (PS) stars in solutions of linear poly(vinyl methyl ether) (PVME), as a function of PS molecular weight and PVME concentration. In these experiments the PS is present in very small amounts, and the PVME is isorefractive with the solvent, *o*-fluorotoluene. Under these conditions, the observed autocorrelation function of the scattered electric field intensity has been shown to reflect the translational diffusion of the PS component, both in principle and in practice<sup>12-14</sup>. Furthermore, the compatibility of the two polymer components increases the probability that the observed diffusion behaviour reflects the same mechanism(s) that operate in binary solutions. The PVME molecular weight was  $1.4 \times 10^5$ , and the PVME concentration covered the range from 0.01 to 0.30 g ml<sup>-1</sup>.

## EXPERIMENTAL

### Dynamic light scattering apparatus

Data were acquired on a dynamic light scattering spectrometer designed and constructed in this laboratory. Radiation at 514.5 nm from an argon-ion laser (Lexel 95-1) is focused into the sample volume by a planoconvex lens ( $f=250$  mm). Scattered radiation is collected through a pinhole-lens-pinhole optical train. The first pinhole, diameter 400  $\mu$ m, acts as an aperture stop to limit the angular acceptance. The biconvex lens,  $f=200$  mm, images the sample volume onto the second pinhole, diameter 200  $\mu$ m, to illuminate approximately two coherence areas on the detector. The photomultiplier tube (EMI 9863A) was hand-selected for low afterpulsing and low dark current; at room temperature the average dark current is approximately 30 counts per second. The detection optics sit on an arm rigidly mounted to a 0.48 m diameter goniometer (Enco 73123) to provide angle selectability. Photon counts pass through an amplifier/discriminator to the autocorrelator (Brookhaven Instruments BI2030). The correlator has 16 channels, which may be multiplexed or used in a multiple sample-time mode to extend the timescale of the experiment. There are also four delayed channels to provide an experimental estimate of the baseline of the autocorrelation function.

The geometry of the scattering cell compartment is illustrated in Figure 1. The novel feature of this design is the variation of the incident beam elevation prior to entering the scattering cell; this permits the instrument to

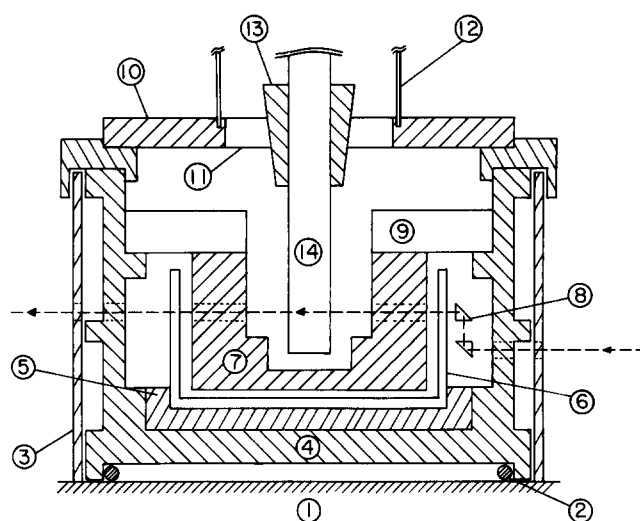


Figure 1 Cross-sectional view of the dynamic light scattering chamber; part numbers are identified in the text

operate with no interference from room light. The beam enters the compartment through a slit in the outer cylinder (3); this cylinder is rigidly mounted to the goniometer, and rotates with the detection arm. The beam then passes through a small aperture in the inner cylinder (4), which is rigidly mounted to an optical table via a 2.54 cm diameter steel shaft (not shown). The beam elevation is then raised approximately 2 cm by a pair of antireflection-coated prisms (8). The beam passes through a flat window cemented into the wall of a polished quartz vat (6) (Brookhaven Instruments BIQVC) which contains index-matching fluid. The transmitted beam is collected by a beam stop (not shown) in the vat. The scattered beam exits through a slit in the inner cylinder and a small aperture in the outer cylinder. A baffle on the outer surface of the inner cylinder effectively prevents any stray light that enters through the outer cylinder slit from reaching the outer cylinder exit port.

The sample solutions are contained in 12 mm o.d. Pyrex cells (14), which are reproducibly centred via a Teflon cone (13). Once in position, the scattering volume may be inspected visually through an annular window (11); room light is excluded by a cap (12). Temperature control is achieved by circulating fluid through a copper block (7) immersed in the index-matching fluid. A thermistor, also immersed in the index-matching fluid within 1 cm of the sample cell, is used to monitor the temperature. During the course of these experiments the temperature was maintained at  $30.0 \pm 0.1^\circ\text{C}$ . The quartz vat is supported on a plastic ring (5), and the copper block on a Plexiglas annulus (9), for thermal isolation.

Alignment of the optics is achieved with the aid of a Filar micrometer microscope and a section of 0.2 mm diameter nylon filament. The microscope is mounted in place of the photomultiplier, and the pinholes replaced by 1 mm apertures. The sample cell is replaced by a 12 mm o.d. aluminium cylinder with the nylon filament stretched taut, on axis, over a 2 cm section at the approximate elevation of the light beam. By reading the relative position of the filament across the field of view of the microscope as the detection arm is rotated, it is possible to extract the coordinates of the filament axis relative to the true rotation centre of the goniometer, by regression

analysis; furthermore, the correct orientation of the detection apertures is established at the same time. The position of the sample holder is then translated in the horizontal plane via set screws in the top plate (10), until the filament is centred to better than 0.001 inch in any direction. The alignment of the laser beam is checked by examining the symmetry of the far-field diffraction pattern with the filament in place. The position of 0° scattering angle is determined with the photomultiplier in place but the beam stop removed, by locating the intensity maximum of an attenuated beam.

#### Samples and solutions

The synthesis and characterization of the 12-arm star polystyrenes have been described<sup>15</sup>. The sample designations and values of  $M_w$  are: PS-9-12,  $5.5 \times 10^4$ ; PS-4-12,  $4.67 \times 10^5$ ; PS-7-12,  $1.11 \times 10^6$ ; PS-10-12,  $1.69 \times 10^6$ . In all cases,  $M_w/M_n$  was less than 1.1. The poly(vinyl methyl ether) synthesis, fractionation and characterization have been reported<sup>16</sup>; for this fraction,  $M_w = 1.4 \times 10^5$ , and  $M_w/M_n$  is approximately 1.6. The solvent, *o*-fluorotoluene (*o*FT), was used as received (Aldrich).

Sample solutions were prepared by filtering appropriate amounts of dilute PS/*o*FT and PVME/*o*FT solutions directly into the scattering cells. For molecular weights below  $10^6$ , 0.22  $\mu\text{m}$  Millipore filters were used, while for the larger samples the pore size was 0.45  $\mu\text{m}$ . The solvent was filtered repeatedly through 0.05  $\mu\text{m}$  filters, prior to use. The resulting sample solution, typically about 5 ml, was then mixed gently but persistently. To achieve the desired starting concentration of PVME, solvent was evaporated very slowly, under a steady flow of dry, filtered nitrogen. Great care was taken to ensure that no polymer was deposited on the walls of the cell; in some instances, it was necessary to add more filtered *o*FT to redissolve adsorbed polymer, and re-evaporate the solvent. PVME is quite sensitive to oxidative degradation, so elevated temperatures could not be used to accelerate the evaporation. Small quantities of antioxidant were also used to inhibit degradation. None of the solutions used exhibited more than a trace of the strong yellow colour indicative of the degradation products. As the PVME sample was not monodisperse originally, it was felt that a small amount of degradation could be tolerated. Analysis of both colourless and yellow PVME solutions revealed that the amount of degradation corresponding to a slight but visible yellowing was chromatographically undetectable.

The scattering cells were scrupulously cleaned and dusted prior to use. Each cell was capped with a ground-glass stopper to permit subsequent dilution. All concentrations were determined gravimetrically. The initial solutions were evaporated down to a volume of approximately 1 ml, corresponding to a PVME concentration near 0.30 g ml<sup>-1</sup>. The concentration of the dilute, binary PS/*o*FT solution was designed to yield a final PS concentration of  $0.1c_{\text{PS}}^*$ , where  $c_{\text{PS}}^*$  in this case refers to the coil overlap concentration in binary PS/*o*FT solutions. Subsequent dilutions were performed by adding filtered stock PS/*o*FT solution, to maintain  $c_{\text{PS}}$  reasonably constant while  $c_{\text{PVME}}$  was varied. There was therefore some fluctuation in  $c_{\text{PS}}$  from dilution to dilution. For PS-9-12, the mean value of  $c_{\text{PS}}$  was 10.7 mg ml<sup>-1</sup>, and the range was  $\pm 0.2$ . For PS-4-12, PS-7-12 and PS-10-12,

the corresponding values were  $2.62 \pm 0.07$ ,  $1.05 \pm 0.1$  and  $0.62 \pm 0.01$  mg ml<sup>-1</sup>, respectively. After each dilution, it was necessary to wait a sufficient time for the solutions to become homogeneous. This interval varied from several weeks at the higher PVME concentrations to a few days in dilute solutions. Homogeneity was confirmed by making the light scattering measurements repeatedly at one week intervals, and also as a function of position in the cell, until no significant variation in the decay rate was found. Between measurements, all solutions were stored in the dark, under a dry nitrogen atmosphere. This entire solution preparation protocol is quite time-consuming, but is necessitated by the limited amounts of PVME fractions available, and the susceptibility to degradation of the PVME.

#### Data acquisition and analysis

For each solution, correlation functions were obtained at six different scattering angles, ranging from 45° to 120°. Sample times were chosen to provide approximately four e-folds in the decay, in the homodyne mode. The last 32 channels were spaced at twice the sample time of the first 96, using the multiple sample time option on the correlator. The experimental baseline was determined by averaging the counts in four additional channels, which were delayed by 1029 times the sample time of the 128th channel. The mean decay rate,  $\Gamma$ , was extracted from the autocorrelation function by cumulant analysis, using the experimental baseline values. In general, a cumulant expansion with two terms was sufficient to extract  $\Gamma$  reliably. Use of theoretical or floating baselines did not have a substantial effect on the values of  $\Gamma$  obtained. It has been pointed out in some detail that cumulant analysis may not be appropriate for concentrated isorefractive solutions, where the molecular weight dependence of  $\Gamma$  is much stronger than in dilute solution<sup>17</sup>, even for very small polydispersities (i.e. 1.05–1.10). However, for all the solutions examined here, the magnitude of the apparent molecular weight exponent for diffusion  $\beta$  ( $D \sim M^\beta$ ) did not exceed 1.1, and there was no evidence of inadequacy in the cumulant fits to the data.

## RESULTS AND DISCUSSION

The relatively low molecular weights of the star arms and the matrix, coupled with the high degree of branching, suggest that these systems might be closer to the second of the two limiting situations identified in the introduction, namely that of a spherical Brownian particle diffusing in a polymer solution. Measurements of coil dimensions and intrinsic viscosity for 12-arm stars support this picture<sup>18</sup>. In the simplest case, where the probe is much larger than the matrix polymer, the diffusion should follow the Stokes–Einstein (SE) prediction at all matrix concentrations,  $c$ ; in other words, the changing concentration only affects diffusion through the macroscopic solution viscosity,  $\eta$ :

$$D = kT/6\pi\eta(c)R = D_0\eta(0)/\eta(c) \quad (1)$$

where  $R$  is the particle radius and  $D_0$  its diffusion coefficient at infinite dilution. In Figure 2, the data are plotted logarithmically as  $D/D_0$  versus matrix concentration; the data are also listed in Table 1. Reduction to a master curve is not observed, and the straightforward SE equation does not apply. The data for

the three largest stars may appear to be close to superposing, but this is only due to the low resolution of a log-log plot. In Figure 3, these data are replotted as  $\log D$  versus  $\log M$ , at several selected concentrations ( $D$  and  $M$  refer exclusively to the PS component). The crucial point here is that the apparent molecular weight exponent  $\beta$  decreases systematically from about  $-0.6$  at low concentration to  $-1.1$  at the highest concentration measured; in the SE limit,  $\beta$  must be independent of concentration. However, these data should not necessarily be interpreted as indicating that the diffusion coefficient obeys an expression of the form  $D \sim M^{\beta(c)}$ , even though such a power-law dependence has been reported for linear PS in a PVME matrix<sup>19</sup>. First, the range of  $M$  shown is quite small; secondly, the lowest  $M$  data (not shown on this plot) fall consistently above extrapolations of the lines in Figure 3, except at infinite dilution; and thirdly, there is some evidence of systematic curvature in the data at each finite PVME concentration in Figure 3. It should also be noted that the  $D$  values plotted in Figure 3

are not in fact identical to the measured values. The actual PVME concentrations employed varied slightly from star to star, and thus the effect of the strong concentration dependence apparent in Figure 2 must be taken into account. This was achieved by using  $D$  values interpolated to the indicated concentrations via the functional form to be discussed subsequently.

The argument advanced above, i.e. that even the three highest molecular weight stars do not follow the SE prediction, assumes that in each case the presence of the star does not affect the bulk solution properties in a significant way, and in a way which varies with star molecular weight and concentration. The low PS concentrations guarantee that the macroscopic solution viscosity is determined only by the PVME concentration. However, it is also possible that  $R$  for the PS component is a function of PVME concentration, thus in effect making  $D_0$ , when used as a normalization constant, a

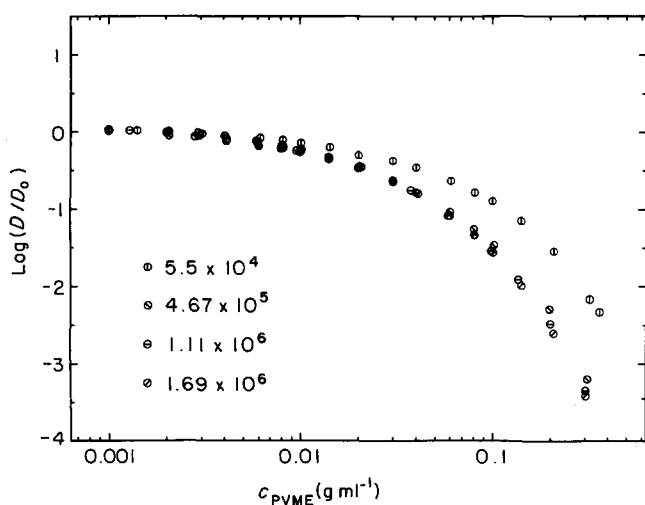


Figure 2 Reduced PS 12-arm star diffusion coefficients as a function of PVME concentration, at  $P = 1.4 \times 10^5$

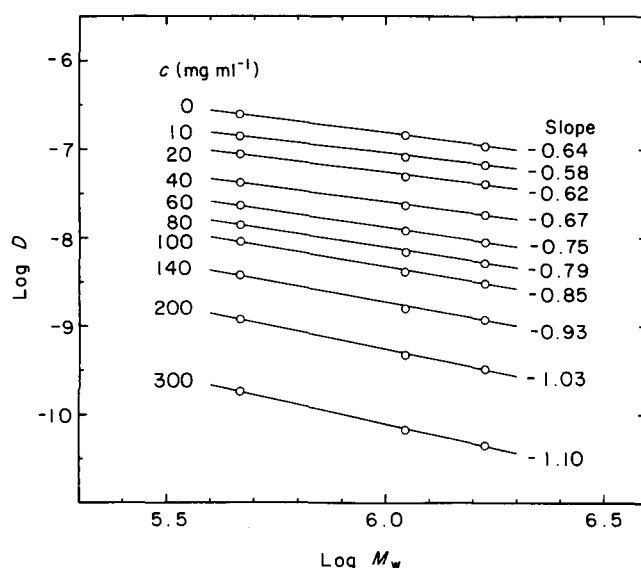


Figure 3 PS diffusion coefficients as a function of PS molecular weight for the three larger stars, at selected PVME concentrations

Table 1 PS diffusion coefficients in PVME solutions,  $P = 1.4 \times 10^5$

$M = 5.5 \times 10^4$		$M = 4.67 \times 10^5$		$M = 1.11 \times 10^6$		$M = 1.69 \times 10^6$	
$\log c^a$	$\log D^a$	$\log c$	$\log D$	$\log c$	$\log D$	$\log c$	$\log D$
-2.993	-6.10	-2.996	-6.58	-2.993	-6.81	-3.002	-6.90
-2.853	-6.11	-2.845	-6.61	-2.891	-6.83	-2.858	-6.91
-2.695	-6.14	-2.689	-6.63	-2.700	-6.85	-2.688	-6.93
-2.534	-6.15	-2.554	-6.65	-2.528	-6.88	-2.517	-6.97
-2.399	-6.16	-2.389	-6.70	-2.387	-6.92	-2.397	-7.00
-2.216	-6.19	-2.221	-6.76	-2.226	-6.98	-2.234	-7.06
-2.095	-6.23	-2.095	-6.80	-2.090	-7.04	-2.098	-7.12
-2.000	-6.26	-2.006	-6.85	-2.021	-7.08	-1.997	-7.17
-1.847	-6.33	-1.855	-6.94	-1.853	-7.18	-1.857	-7.27
-1.698	-6.41	-1.697	-7.05	-1.698	-7.30	-1.686	-7.40
-1.522	-6.50	-1.395	-7.38	-1.520	-7.50	-1.522	-7.58
-1.399	-6.59	-1.220	-7.62	-1.428	-7.60	-1.391	-7.75
-1.221	-6.76	-1.095	-7.85	-1.222	-7.92	-1.229	-8.04
-1.095	-6.91	-0.990	-8.06	-1.093	-8.17	-1.095	-8.29
-1.001	-7.02	-0.854	-8.41	-1.002	-8.39	-0.998	-8.52
-0.845	-7.28	-0.706	-8.89	-0.865	-8.76	-0.848	-8.95
-0.682	-7.67	-0.512	-9.79	-0.700	-9.34	-0.683	-9.56
-0.498	-8.28			-0.519	-10.19	-0.514	-10.36
-0.447	-8.46						

<sup>a</sup> Units:  $c$ ,  $\text{g ml}^{-1}$ ;  $D$ ,  $\text{cm}^2 \text{s}^{-1}$

function of PVME concentration. The precise effect of increasing PVME concentration on the star coil dimensions is as yet unknown, although some reasonable inferences can be made on the basis of these and other diffusion data in the same chemical system. However, it is clear that if the stars are modelled as effective spheres, and if their radii vary with PVME concentration, quantitative interpretation of the results will need to account for this. One possibility would be a contraction of the average star dimensions with increasing matrix concentration, as observed in binary linear polymer solutions<sup>20</sup>. Such a contraction might also be a weakly increasing function of star molecular weight, i.e. a greater contraction for larger  $M$ , to reflect the  $M$  dependence of the dilute-solution Flory expansion coefficient. However, the resulting deviation from Equation (1) would be in the direction opposite to that evident in Figure 2, i.e.  $D/D_0$  values for the larger stars would lie above those of the smaller. Thus, the conclusion that the data of Figures 2 and 3 indicate a definite departure from SE behaviour is well supported.

The values of  $D_0$  utilized in Figure 2 were obtained by extrapolation to infinite dilution of diffusion coefficients measured in dilute PS/oFT solutions. The corresponding hydrodynamic radii for the four stars thus obtained were 5.0, 15, 26 and 33 nm, for PS-9-12, PS-4-12, PS-7-12 and PS-10-12, respectively, which are in close agreement with those reported for the same stars in toluene<sup>15</sup>. This supports the consideration of oFT as a good solvent for PS, in accordance with data on linear and three-arm polystyrenes<sup>8,19</sup>. The interesting question, raised previously, is how or whether the average star dimensions vary with matrix concentration. If the compatibility of PS and PVME in oFT is such that a PS monomer cannot distinguish between PS and PVME monomers ( $\chi_{\text{PS-PVME}} = 0$ ), then the addition of PVME to solution should cause a gradual contraction of the PS coils towards the unperturbed, melt dimensions. On the other hand, finite  $\chi_{\text{PS-PVME}}$  values might preserve excluded-volume interactions in the PS stars at all PVME concentrations. In the former case,  $D_0$  would not provide an appropriate normalization at all PVME concentrations. The situation is more complicated than this, however, because a finite PS concentration is always used. The diffusion coefficient measured by dynamic light scattering can be written as

$$D_{\text{PS}} = D_0(1 + k_D c_{\text{PS}} + \dots)f \quad (2)$$

where  $f$  is the unknown function describing the concentration, molecular weight and topology dependence of diffusion, and  $k_D$  accounts for the finite PS concentrations necessary to perform the experiment. Thus, in principle both  $D_0$  and  $k_D$  can depend on  $M$ , matrix concentration and perhaps also matrix molecular weight. Preliminary measurements on linear polystyrenes in PVME/oFT solutions suggest that indeed  $k_D$  decreases from its typical good solvent values in binary PS/oFT solutions as  $c_{\text{PVME}}$  is increased<sup>19</sup>. Furthermore, for linear PS, reduction of  $D/D_0$  versus  $c_{\text{PVME}}/c_{\text{PS}}^*$  to a master curve was not observed unless  $c_{\text{PS}}^*$  was estimated assuming that the ternary solution was an effective theta solvent. Extensive, direct measurements of both static coil dimensions and  $k_D$  as functions of  $c_{\text{PVME}}$  are in progress, but are quite time-consuming; thus, at this stage it is not possible to determine the 'correct'  $D_0$  to use in plots such as Figure 2. Based on the relative values of  $D_0$  reported in binary polystyrene/toluene and polystyrene/cyclohexane

solutions<sup>15</sup>, the effective hydrodynamic radius could decrease by as much as 40% for the largest PS star over the  $c_{\text{PVME}}$  range studied, which could have a significant effect on plots such as Figure 2. This estimate assumes that the PS coils do not contract any more than they would in a theta solvent, which is reasonable because no evidence of aggregation, precipitation or microphase separation of the PS component has been observed in these solutions.

The mobility of Brownian particles in various kinds of matrix has received considerable attention since the pioneering work of Brinkmann<sup>21</sup> and Debye and Bueche<sup>22</sup>. There have been several more recent treatments of this problem, with relevance to the data reported here<sup>23-29</sup>. Similarities and differences between these approaches have been summarized elsewhere<sup>3</sup>, but the essential result is that diffusion should be describable by an equation of the form

$$D/D_0 = \exp(-kR) \quad (3)$$

where  $k$  is a concentration-dependent parameter and  $R$  is the particle radius. In general,  $k$  has a power-law dependence on concentration, with exponent  $u = 0.5^{28}$ ,  $0.75^{27}$  or  $1.0^{25,26}$ . Although in most treatments the form of Equation (3) arises from the presence of spatially fixed obstacles in the solution, which serve to generate screening of hydrodynamic interactions, whereas the data concern solutions of flexible polymers, experimental results are consistent with this functional form. However, strong differences exist among the data in the exact relationships observed between molecular properties and fitting parameters. Equation (3) may be written in an expanded form as suggested by Phillies<sup>3</sup>:

$$D/D_0 = \exp(-ac^u R^v P^w) \quad (4)$$

where  $P$  is the matrix polymer molecular weight. Langevin and Rondelez<sup>30</sup> have reported sedimentation results for various particles in poly(ethylene oxide) solutions which are consistent with  $w = 0$  and  $u$  between 0.5 and 0.65, although their interpretation with respect to  $w$  has been questioned<sup>3</sup>. The result  $w = 0$  is to be expected if the scaling picture of semi-dilute solutions is correct, i.e. if  $D/D_0$  can be written as a function of the dimensionless ratio  $R/\xi$ , where  $\xi$  is the screening length. Furthermore, in this case an explicit relationship between  $u$  and  $v$  exists; namely,  $u = v$  in a theta solvent, and  $u = 0.75v$  in a good solvent. To some extent the sedimentation data were in accordance with this expectation; however, polymer adsorption on the surface of the particles was a severe problem. In addition, for good solvent conditions,  $u = 0.75^{27}$ , so there is some discrepancy on this point. The extensive measurements of Phillies *et al.*<sup>3</sup> on the diffusion of latex spheres in aqueous polymer solutions have been summarized as being consistent with Equation (3), but with  $v = 0$  to  $-0.1$ ,  $w = 0.8 \pm 0.1$  and  $u = 0.6$  to  $1$ . Thus, while the form of Equation (3) is consistent with experiment, there remains a considerable amount of uncertainty about the significance of the parameter values obtained.

In light of the preceding discussion, the measured diffusion coefficients have been fitted to the functional form

$$D = D_0 \exp(-ac_{\text{PVME}}^u) \quad (5)$$

In this instance,  $D_0$  may be selected as an adjustable

meter or the infinite dilution values can be used; both approaches have been taken. In Figure 4 the data are plotted as  $\log D$  versus  $\log c$ , along with the best fit obtained via Equation (5), with  $D_0$  left as a floating parameter. The agreement is extremely good, and the floating values of  $D_0$ ,  $a$  and  $u$  are listed in Table 2. In Figure 5, the data are plotted as  $\log[a^{-1} \log(D_0/D)]$  versus  $\log c$ , where the measured  $D_0$  has been used. Ideally, it would be preferable to use measured values for  $D_0$  to avoid the possibility that  $D_0$  varies with concentration, but the floating  $D_0$  may be at least as valid an approach. The variation between the measured and floating values ranges up to 40%, and increases with star number. Thus this variation falls within the range suggested previously, and is in the 'right' direction, i.e. the higher values of  $D_0$  obtained by floating the parameter are consistent with a contraction of coil size with increasing concentration. The plotting format of Figure 5 minimizes small deviations between experiment and theory, due to the repeated logarithm. The error bars on the effect of a 10% underestimate of  $D_0$  at low concentrations; at high matrix concentrations the potential error bars would not extend beyond the circles representing the data points themselves. However, if the deviation between the data and a straight line in Figure 5 is attributable to changes in coil dimension, then there is some suggestion that the functional form itself is not quite correct, due to the systematic nature of the deviation. The straight line in Figure 5 has a slope of 0.74, an average of the four  $u$  values in Table 2. The values of  $u$  listed in Table 2 range from 0.66 to 0.76 for the floating  $D_0$  fit, and from 0.72 to 0.77 using the measured values. Thus, to some degree the exponent is

independent of diffusing particle and represents a property of the matrix. These values fall in the range between the expected good solvent screening length dependence ( $u=0.75$ ) and that observed by dynamic light scattering ( $u\sim 0.67$ )<sup>31</sup>; they are also consistent with some of the optical probe studies of Phillies<sup>3</sup> and some of the probe sedimentation results of Langevin and Rondelez<sup>30</sup>. The values of  $a$  in Table 2 indicate at most a weak dependence on probe radius  $R$ . By standard scaling arguments the screening length  $\xi$  in these solutions varies from about 10 nm at the overlap concentration down to 2 nm at the highest concentration; thus the ratio  $R/\xi$  ranges from about 0.5 to 16 above the matrix overlap concentration. If the data are compared to the form  $a\sim R^v$ , a value for  $v$  of  $0.2\pm 0.1$  is obtained. This is reminiscent of the results of Phillies, where  $v$  was 0 or even slightly negative; the range of  $R$  is small, however, so this value of  $v$  may not be too accurate. (Furthermore, when  $u$  varies with  $M$ , the values of  $a$  and thus  $v$  obtained depend on the concentration units employed.) Nevertheless, this weak dependence on  $R$  is in disagreement with the assertion that the ratio  $D/D_0$  should follow a scaling law  $D/D_0\sim f(R/\xi)$ . This discrepancy has been ascribed to cooperative motions of probe particle and surrounding polymer<sup>3</sup>, a concept that is extremely difficult to develop in a quantitative manner. Stated in a slightly different way, the mobility of matrix polymer chains may be at least as important as the average mesh size itself in determining diffusion rates. There is a growing body of evidence that this is the case. For example, dynamic light scattering results on the same ternary system, but using

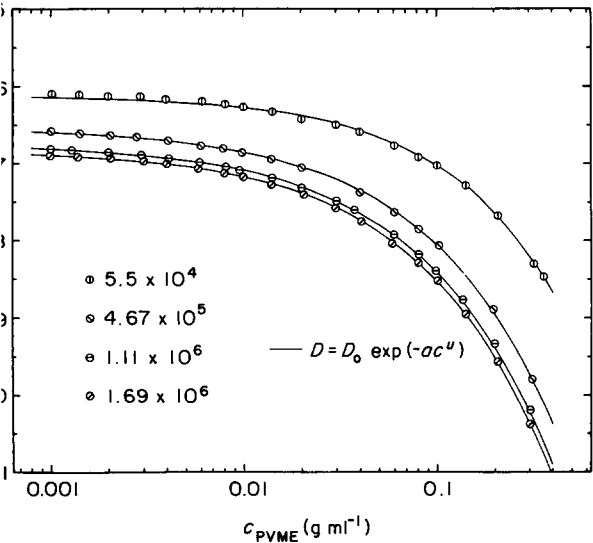


Figure 4 PS diffusion coefficients compared to Equation (5), with  $D_0$  as a floating parameter, at  $P=1.4\times 10^5$

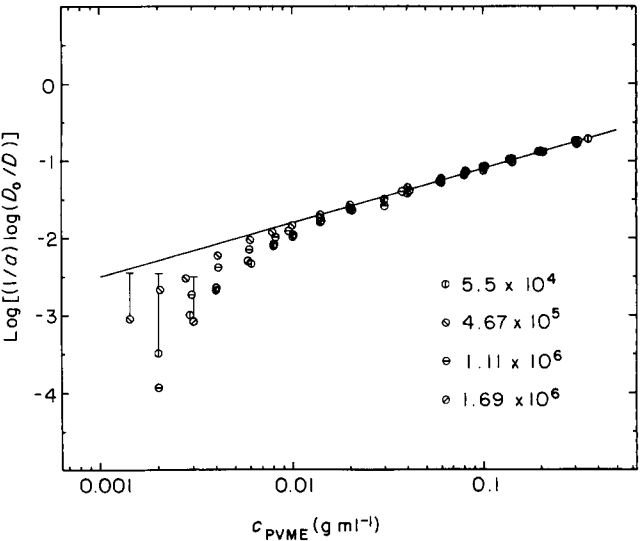


Figure 5 PS diffusion coefficients compared to Equation (5), with  $D_0$  fixed at the measured value, at  $P=1.4\times 10^5$ ; the format has been altered relative to Figure 4 to emphasize the deviation of the data from Equation (5)

Table 2 Fits of PS diffusion coefficients to Equation (5)

	$D_0$ (measured)	$a$	$u$	$D_0$ (floated)	$a$	$u$
$10^4$	$7.33\times 10^{-7}$	0.058	0.77	$7.72\times 10^{-7}$	0.062	0.76
$<10^5$	$2.53\times 10^{-7}$	0.118	0.72	$2.98\times 10^{-7}$	0.159	0.67
$<10^6$	$1.42\times 10^{-7}$	0.121	0.73	$1.91\times 10^{-7}$	0.183	0.66
$<10^6$	$1.10\times 10^{-7}$	0.110	0.75	$1.56\times 10^{-7}$	0.188	0.66

linear diffusing polymers and a considerably larger matrix molecular weight, reveal that even when the reduced matrix concentration  $c/c^*$  reaches 25, a molecular weight exponent of  $-2$  is not observed<sup>19</sup>; the implication is that reptation is not the only available diffusion mechanism. Furthermore, these linear polymer results indicate that a power law  $D \sim M^\beta$  is followed at all matrix concentrations, even though at any single concentration the ratio  $R/\xi$  may vary from less than to greater than unity. Both of these observations are consistent with a matrix mobility greater than the scaling approach considers. In the reptation picture, matrix mobility is taken into account via the constraint release mechanism. Extensive forced Rayleigh scattering measurements in semi-dilute solutions have indicated a matrix molecular weight dependence of diffusion, until the matrix is 3–5 times larger than the diffusant<sup>32</sup>; at first glance, this appears to indicate the importance of constraint release in semi-dilute solutions. However, more detailed examination of this issue reveals that it is not in fact possible to combine reptation and constraint release in a self-consistent manner to describe linear polymer diffusion in semi-dilute solution<sup>19,32</sup>.

As has been discussed in detail in the context of three-arm star diffusion, reptation is the only postulated transport mechanism that considers diffusant topology explicitly<sup>8</sup>. Thus, it is appropriate to compare the results for 12-arm stars reported here with those of linear polymers under comparable conditions, as a way to assess whether reptation, or at least diffusant topology, affects diffusion rates in these solutions. While no data for linear PS in this molecular weight matrix are available, there have been several studies in similar systems. In particular, extensive linear PS data have been reported<sup>19,33</sup> in PVME matrices with  $P = 6 \times 10^4$  and  $1.3 \times 10^6$ . The comparison of branched and linear behaviour is effected by computing the ratio  $D_B/D_L$  as a function of matrix concentration, where  $D_B$  and  $D_L$  are the diffusion coefficients of a 12-arm star and an appropriately chosen linear PS, respectively. In this case, the linear molecule has been selected as having  $M$  equal to one-sixth the star  $M$ . Thus, the linear polymer can be viewed as a two-arm star with an arm molecular weight equivalent to that for the corresponding 12-arm star. This choice of 'span' molecular weight has been shown to be effective in providing reduction of properties of stars of differing functionalities to a master curve<sup>9</sup>. Actual values of  $D_B/D_L$  were computed in the following manner:  $D_B$  was obtained directly from Equation (5), using the parameters in Table 2, while  $D_L$  was obtained by a three-stage procedure. In the first step, data for a linear PS,  $M = 1.79 \times 10^5$ , obtained in the two matrices identified above<sup>19,33</sup>, were interpolated to particular concentrations using Equation (5). These results were then used to interpolate to  $P = 1.4 \times 10^5$ , assuming a power-law dependence on  $P$ . This step was not as drastic as it might appear, because the  $P$  dependence of the diffusion coefficients was not great (i.e. apparent exponents of magnitude less than unity). Finally, these data, corresponding to  $M = 1.79 \times 10^5$  in  $P = 1.4 \times 10^5$ , were scaled to the span molecular weights for the three larger 12-arm stars. The molecular weight scaling was achieved using the relation  $D_L \sim M^\beta$ , where  $\beta$  is a function only of the reduced matrix concentration,  $c/c^*$ ; previously, it was shown<sup>19</sup> that  $\beta$  values obtained from matrices with  $P = 6 \times 10^4$ ,  $1.1 \times 10^5$

and  $1.3 \times 10^6$  collapsed to a master curve when plotted versus reduced matrix concentration  $c/c^*$ . Only the three larger 12-arm stars were considered in this analysis. The resulting values of  $D_B/D_L$  exhibited a smooth decrease with increasing matrix concentration, independent of star molecular weight. However, the decrease was not great; from a matrix concentration of  $0.001 \text{ g ml}^{-1}$  to  $0.20 \text{ g ml}^{-1}$  the ratio decreased by only a factor of 2. This should be contrasted with the equivalent ratio formed for a three-arm star,  $M = 1.19 \times 10^6$ , in a much higher molecular weight matrix,  $P = 1.3 \times 10^6$ ; in that case, the ratio decreased by a factor of 10 over a smaller concentration range<sup>8</sup>. Thus, this admittedly approximate calculation suggests that the effect of topology on diffusion exhibits little dependence on concentration as the solution passes through the semi-dilute regime; by extension, under these solution conditions reptation is probably not important for linear polymers. As a point of reference,  $c^*$  for this matrix is estimated to be  $0.020 \text{ g ml}^{-1}$ , and the entanglement concentration<sup>34</sup>,  $c_e$ , is approximately  $0.10 \text{ g ml}^{-1}$ , using a value<sup>35</sup> of 14 400 for  $P_e$ . At the highest matrix concentration studied here,  $c/c^* \approx 15$ , the value of  $\beta$  was  $-1.5$  for linear polymer diffusion<sup>19</sup>. Thus, the conclusion that reptation is not dominant in this regime is in agreement with the linear polymer results.

## CONCLUSIONS

The technique of dynamic light scattering from ternary solutions has been applied to measure the translational diffusion coefficients of 12-arm star polystyrenes in solutions of linear poly(vinyl methyl ether), as a function of polystyrene molecular weight and matrix concentration. Although the segment density in a 12-arm star is quite high, and to a first approximation the star may be treated as a sphere, the Stokes–Einstein equation for diffusion does not hold in semi-dilute solutions, as has already been observed for the diffusion of latex spheres and colloidal particles in solutions of linear polymers. An empirical, stretched-exponential form is successful in describing the concentration dependence of the data, but the exact parameter values are somewhat uncertain, due to the possibility of contraction of star dimensions with increasing concentration. Nonetheless, the results are not consistent with a simple scaling function,  $f(R/\xi)$ . The timescale for matrix motions is sufficiently rapid that the suppression of reptation by long-chain branching is not important in these solutions, even though the concentrations employed did exceed both the coil overlap concentration  $c^*$  and the entanglement concentration,  $c_e$ . This is in contrast to analogous measurements performed on three-arm stars in a much higher molecular weight matrix. Extension of the 12-arm star measurements to a higher molecular weight matrix is currently under way.

## ACKNOWLEDGEMENTS

Acknowledgement is made to Dr L. J. Fetters for providing the branched polymers, to L. M. Wheeler for assistance in the conduct of the experiments, and to the Donors of The Petroleum Research Fund, administered by the American Chemical Society, for partly supporting this research.

## REFERENCES

- 1 de Gennes, P. G. *J. de Physique* 1975, **36**, 1199
- 2 Klein, J. *Macromolecules* 1986, **19**, 105
- 3 Phillies, G. D. J. *J. Chem. Phys.* 1985, **82**, 5242
- 4 Phillies, G. D. J. *Macromolecules* 1986, **19**, 2367
- 5 Klein, J., Fletcher, D. and Fetters, L. J. *Nature (London)* 1983, **304**, 526
- 6 Bartels, C. R., Crist, B., Jr, Fetters, L. J. and Graessley, W. W. *Macromolecules* 1986, **19**, 785
- 7 Antonietti, M. and Sillescu, H. *Macromolecules* 1986, **19**, 798
- 8 Lodge, T. P. and Wheeler, L. M. *Macromolecules* 1986, **19**, 2983
- 9 von Meerwall, E., Tomich, D. H., Hadjichristidis, N. and Fetters, L. J. *Macromolecules* 1982, **15**, 1157
- 10 von Meerwall, E., Tomich, D. H., Grigsby, J., Pennisi, R. W., Fetters, L. J. and Hadjichristidis, N. *Macromolecules* 1983, **16**, 1715
- 11 Xuexin, C., Zhongde, X., von Meerwall, E., Seung, N., Hadjichristidis, N. and Fetters, L. J. *Macromolecules* 1984, **17**, 1343
- 12 Hanley, B., Balloge, S. and Tirrell, M. *Chem. Eng. Commun.* 1983, **24**, 93
- 13 Lodge, T. P. *Macromolecules* 1983, **16**, 1393
- 14 Martin, J. E. *Macromolecules* 1984, **17**, 1279
- 15 Huber, K., Burchard, W. and Fetters, L. J. *Macromolecules* 1984, **17**, 541
- 16 Bauer, B. J., Hanley, B. and Muroga, Y. *Polymer* submitted
- 17 Lodge, T. P., Wheeler, L. M., Hanley, B. and Tirrell, M. *Polym. Bull.* 1986, **15**, 35
- 18 Roovers, J., Hadjichristidis, N. and Fetters, L. J. *Macromolecules* 1983, **16**, 214
- 19 Wheeler, L. M., Lodge, T. P., Hanley, B. and Tirrell, M. *Macromolecules* 1987, in press
- 20 Daoud, M., Cotton, J. P., Farnoux, B., Jannink, G., Sarma, G., Benoit, H., Duplessix, R., Picot, C. and de Gennes, P. G. *Macromolecules* 1975, **8**, 804
- 21 Brinkmann, H. C. *Appl. Sci. Res.* 1947, **A1**, 27
- 22 Debye, P. and Bueche, A. J. *J. Chem. Phys.* 1948, **16**, 573
- 23 Laurent, T. C. and Pietruszkiewicz, A. *Biochim. Biophys. Acta* 1961, **49**, 258
- 24 Ogston, A. G., Preston, B. N. and Wells, J. D. *Proc. R. Soc. Lond. A* 1973, **333**, 297
- 25 Freed, K. F. and Edwards, S. F. *J. Chem. Phys.* 1974, **61**, 3626
- 26 Freed, K. F. and Edwards, S. F. *J. Chem. Soc. Faraday Trans. II* 1975, **71**, 2025
- 27 de Gennes, P. G. *Macromolecules* 1976, **9**, 594
- 28 Cukier, R. I. *Macromolecules* 1983, **17**, 252
- 29 Altenberger, A. R., Dahler, J. S. and Tirrell, M. *J. Chem. Phys.* 1986, **84**, 5122
- 30 Langevin, D. and Rondelez, F. *Polymer* 1978, **19**, 875
- 31 Adam, M. and Delsanti, M. *Macromolecules* 1977, **10**, 1229
- 32 Kim, H., Chang, T., Yohanan, J. M., Wang, L. and Yu, H. *Macromolecules* 1986, **19**, 2737
- 33 Hanley, B., Tirrell, M. and Lodge, T. P. *Polym. Bull.* 1985, **14**, 137
- 34 Ferry, J. D. 'Viscoelastic Properties of Polymers', 3rd Edn., Wiley, New York, 1980
- 35 Hashimoto, T., Itakwa, M. and Shimidzu, N. *J. Chem. Phys.* 1986, **85**, 6773